

## Period-Adding Phenomenon in a Model of Chemical System

Francesca Aicardi

*International School for Advanced Studies,  
34014 Trieste, Italy*

Andrzej Lech Kawczynski

*Institute of Physical Chemistry, Polish Academy of Sciences,  
01224 Warsaw, Poland*

**Abstract.** A continuous dynamical system is presented in which the period-adding phenomenon is observed when a bifurcation parameter is changed. This phenomenon is characterized by a family of one-dimensional return maps of a cusp shape which exhibits a saddle-node bifurcation.

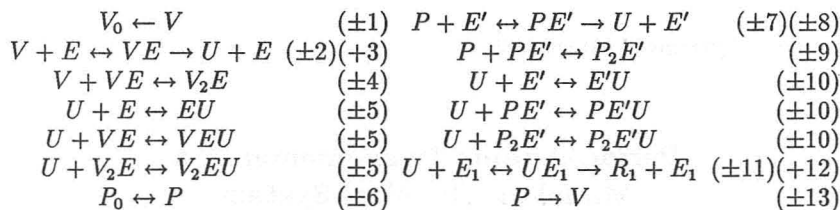
### 1. Introduction

The behavior of some dynamical systems can be characterized by one-dimensional unimodal return maps which have a cusp shape form [1-4]. The typical phenomenon which appears for such types of maps is the so-called period adding [5,6]. When a bifurcation parameter is changed in such a way that one of the branches of the map tends to tangency with the diagonal (a saddle-node bifurcation), a sequence of attracting periodic orbits appears: an  $n$ -periodic orbit is followed by an  $(n + 1)$ -periodic orbit for  $n$  going to infinity.

In this paper we present a model of a continuous dynamical system in which the period-adding phenomenon appears. This model has been investigated earlier but the sequence of bifurcations obtained did not agree with known scenarios [4]. We will show that the bifurcations sequence can be described by a family of one-dimensional return maps with a cusp shape.

### 2. Model

The model describes an open chemical system with coupled enzymatic reactions. The chemistry of the model is described by the following reactions scheme. Only elementary reactions (mono- and bimolecular excluding autocatalytic steps) occur. The numbers on the right-hand side numerate rate constants of respective reactions.



The scheme describes two coupled enzymatic reactions with enzymes  $E$  and  $E'$ , in which two different substrates  $V$  and  $P$  are transformed to the same product  $U$ . Each of these reactions is inhibited by an excess of its own substrate and the common product. It is assumed that rate constants for the allosteric inhibition by product do not depend on how many molecules of the product are present in the enzyme-product complex. The system is open for substrates  $V$  and  $P$  due to reactions  $(\pm 1)$  and  $(\pm 6)$  (concentrations of  $P_0$  and  $V_0$  are kept constant). The irreversible outflow of the product  $U$  is realized by another enzymatic reaction  $(\pm 11)$  and  $(+12)$ . Further, it is assumed that this reaction proceeds in its saturation regime. The inhibition of the two first enzymatic reactions together with the irreversible transformation of  $P$  to  $V$  create the desired coupling inside the scheme. Such coupling can be useful in the modeling of time evolution of metabolites, which are produced in two or more metabolic pathways.

Rates of the reactions follow mass-action law. To simplify the description of the dynamical behavior of the system, it is assumed that total concentrations of all enzymes are much lower than concentrations of substrates and product. With this assumption, the concentrations of all enzymes and all their complexes with substrates and product become fast variables. In a slow time scale (appropriate for the description of changes of substrates and product), they are determined by their quasi-stationary values and can be eliminated from kinetic equations using the Tikhonov theorem [7]. The dynamical behavior of the system is then described by three kinetic equations. In dimensionless form they are given by

$$\frac{dv}{dt} = A_1 - A_2v - \frac{v}{(1+v+A_3v^2)(1+u)}$$

$$\begin{aligned} \frac{du}{dt} = \epsilon_2 \left( \frac{v}{(1+v+A_3v^2)(1+u)} + B \left( \frac{p}{(1+p+B_3p^2)(1+Ku)} \right) \right. \\ \left. + Dp - \frac{Cu}{L+u} \right) \end{aligned}$$

$$\frac{dp}{dt} = \epsilon_3 \left( B_1 - B_2p - B \left( \frac{p}{(1+p+B_3p^2)(1+Ku)} \right) \right)$$

where  $v = [V]/K_m$ ,  $p = [P]/K'_m$ ,  $u = K_5[U]$  are dimensionless concentrations of  $V$ ,  $P$ , and  $U$ , and  $t = t'(k_3 E_0/K_m)$  is dimensionless time ( $t'$  is real time). The values of the parameters are defined as follows:

$$K_m = \frac{k_{-2} + k_3}{k_2}, \quad K'_m = \frac{k_{-7} + k_8}{k_7}, \quad K_{m1} = \frac{k_{-11} + k_{12}}{k_{11}}, \quad K_i = \frac{k_i}{k_{-i}}$$

for  $i = 4, 5, 9, 10$ ,

$$A_1 = \frac{k_1[V_0]}{k_3 E_0}, \quad A_2 = \frac{k_1 K_m}{k_3 E_0}, \quad A_3 = K_4 K_m,$$

$$B = \frac{k_8 E'_0}{k_3 E_0}, \quad C = \frac{k_{12} E'_0}{k_3 E_0}, \quad D = \frac{k_{13} K'_m}{k_3 E_0},$$

$$B_1 = \frac{k_6[P_0]}{k_3 E_0}, \quad B_2 = \frac{k_{-6} K'_m}{k_3 E_0}, \quad B_3 = K_9 K'_m,$$

$$K = \frac{K_{10}}{K_5}, \quad L = K_5 K_{m1}, \quad \epsilon_2 = K_m K_5, \quad \epsilon_3 = \frac{K_m}{K'_m}$$

where  $E_0$  and  $E'_0$  are the total concentrations of enzymes  $E$  and  $E'$ .

Some geometrical arguments concerning qualitative properties of trajectories are given elsewhere [4].

### 3. Results

We have assumed the same values of the parameters as in the previous work [4] (however, results analogous to those shown here can be obtained also with the values approximated to the fourth decimal digit):

$$\begin{aligned} A_1 &= 0.08928606601, & A_2 &= 0.01486767767, & A_3 &= 4, & B &= 0.04, \\ B_1 &= 0.000701754, & B_2 &= 0.000140351, & B_3 &= 4, & C &= 0.122, \\ D &= 0.001, & K &= 10, & L &= 0.74 & \text{and } \epsilon_2 &= 0.2. \end{aligned}$$

$\epsilon_3$  plays the role of bifurcation parameter. We change  $\epsilon_3$  within the interval (1.28, 1.36).

One can roughly characterize periodic as well as chaotic orbits by a sequence of small ( $S$ ) and large ( $L$ ) loops or short and long ones respectively. Looking at the coordinate  $u(t)$  along the orbit, one can see that it has local maxima at approximately the same level (1.45 – 1.5) and local minima at two different levels (the first at about 1.1 – 1.4 and the second at about 0.7 – 0.8). Small (short) loops correspond to maximum — upper minimum — maximum, whereas large (long) loops correspond to maximum — lower minimum — maximum.

At  $\epsilon_3 = 1.28$ , the system approaches the periodic trajectory with the sequence  $SSL$  for all initial conditions, whereas at  $\epsilon_3 = 1.36$  the periodic trajectory with the sequence  $SSLSSL$  is the sole attractor. Examples of attracting periodic trajectories are shown in figure 1.

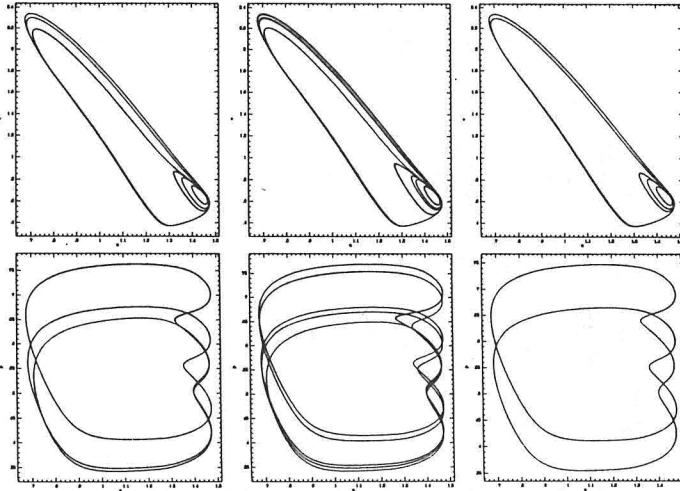


Figure 1: Projections of attracting periodic trajectories on the planes  $(u, v)$  and  $(u, p)$  for given values of  $\epsilon_3$ : (a)  $\epsilon_3 = 1.36$  — the stable  $SSLSSL$ -periodic orbit, (b)  $\epsilon_3 = 1.34$  — the first adding of the sequence  $SSL$  to the  $SSLSSL$ -periodic orbit is seen. The  $SSLSSL(SSL)$ -periodic orbit is attracting. (c)  $\epsilon_3 = 1.28$  — the stable  $SSL$ -periodic orbit.

To characterize the behavior of the system, we made the Poincaré section at the plane  $u = 1.4343$ , looking only at those cases when trajectories cross this plane with  $u(t)$  decreasing. Examples are shown in figure 2.

The apparent one-dimensionality of the Poincaré sections is caused by the very strong contraction of trajectories in one direction. All points of the cross sections lie along (almost straight) three lines. The far-left line consists of points belonging to large loops. All remaining points belong to small loops. The number of lines is determined by the longest subsequence of successive small loops ( $SSL$  in the considered range of  $\epsilon_3$ ). This is equal to the number of successive small loops plus one, as large loops form the far-left line.

The first return diffeomorphism  $F_{\epsilon_3}$  gives the following picture. Subsequent iterations belong to small loops, provided the value of  $p$  increases, whereas those with decreasing value of  $p$  always belong to large loops. The sequence  $SL$  consists of one “jump” with increasing value of  $p$  belonging to a subsequent line starting from the left one, followed by “jump” with decreasing values of  $p$  belonging to the far-left line. The sequence  $SSL$  consists of two small loops with increasing  $p$  followed by a large loops with decreasing  $p$ .

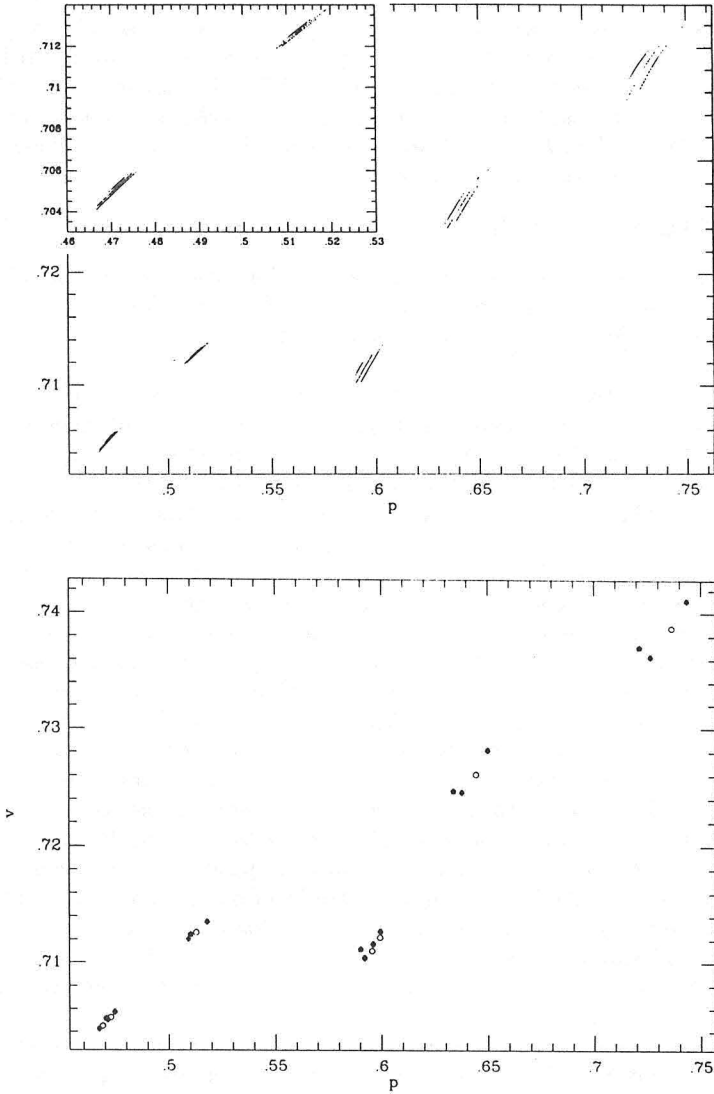


Figure 2: The Poincaré sections at the plane  $u = 1.4343$  for given values of  $\epsilon_3$ . Five sets of points  $I_1, I_2, I_3, I_4, I_5$  are seen. (a) The most left sets  $I_1, I_2, I_3, I_4, I_5$  correspond to  $\epsilon_3 = 1.287$ , the middle to  $\epsilon_3 = 1.301$ , and the most right to  $\epsilon_3 = 1.32$ . In these cases the trajectories seem to be chaotic. In the window the enlargement of  $I_1$  and  $I_2$  is shown. (b)  $\epsilon_3 = 1.28$  (black pentagons),  $\epsilon_3 = 1.34$  (stars), and  $\epsilon_3 = 1.36$  (white heptagons). The corresponding periodic trajectories are shown in figure 1.

For all  $\epsilon_3$ , points belonging to the far-left line “jump” to the next middle line and points belonging to the far-right line “jump” to the far-left line, whereas points belonging to the middle line can “jump” with increasing value of  $p$  to the subsequent right line or they can “jump” with decreasing  $p$  to the far-left line. The Poincaré sections look like a union of five disjoint sets. Counting from the left to the right let us call them:  $I_1, I_2, I_3, I_4, I_5$ . The sets  $I_1$  and  $I_2$  belong to the left line,  $I_3$  and  $I_4$  belong to the middle line, and  $I_5$  belongs to the right line. It is seen that for all  $\epsilon_3$

$$F(I_1) \subset I_3, F(I_2) \subset I_4, F(I_3) \subset I_1 \cup I_5, F(I_4) \subset I_1 \text{ and } F(I_5) \subset I_2.$$

In some subintervals of  $\epsilon_3$  the Poincaré sections contain finite numbers of points in each set. In these windows trajectories are periodic. Outside of the windows trajectories seem to be chaotic. The Poincaré sections seem to contain infinite numbers of points in each set.

Let us notice that at a given  $\epsilon_3$ , the trajectory intersects the plane  $u = 1.4343$  at different values of coordinate  $p$ . So, one can use the changes of this coordinate (at the Poincaré section) with  $\epsilon_3$  to characterize the appearing bifurcations. In order to avoid transient behavior, some initial intersections are omitted. The results of numerical calculations are shown in figure 3.

The values of  $p$  at intersections are grouped into five bunches corresponding to the five sets seen in Poincaré sections. The windows where trajectories are periodic are clearly seen. They are separated by intervals of  $\epsilon_3$  where trajectory is chaotic. Going with  $\epsilon_3$  from right to left, we see that one additional intersection appears in each of the five bunches of  $p$  values. This corresponds to the appearance of the new subsequence  $SSLSL$ , which is added to the previous sequence  $SSLSLSL(SSLSL)_n$  describing periodic trajectory.

We can parametrize a bunch by coordinate  $p$  and induce a one-dimensional return map on this bunch. In this way, a map of the interval of  $p$  to itself is constructed. In figure 4, examples of maps for different  $\epsilon_3$  are shown.

They are all the cusp-shape type. They are continuous, but the derivative at maximum changes discontinuously from large positive to large negative. With  $\epsilon_3$  decreasing, the left branch of the family of maps changes its position and tends to tangency with the diagonal. The change of  $\epsilon_3$  is accompanied by the period adding. A new attracting orbit appears with one more fixed point for appropriate iterate of the map when we go to the left, from one window to the next.

With decreasing  $\epsilon_3$  in the interval  $(1.28, 1.36)$  the sequence  $SSLSL$  appears more and more frequently in the attracting periodic trajectories. At the tangency of the left branch with the diagonal ( $\epsilon_{3,t} = 1.28562\dots$ ), the sequence  $SSLSLSL$  disappears and the sequence  $SSLSL$  remains the only one and composes the attracting periodic trajectory.

#### 4. Discussion

The family of the first return diffeomorphism  $F_{\epsilon_3}$  seems to be of the Hénon type and therefore hard to analyze quantitatively. However, the complex

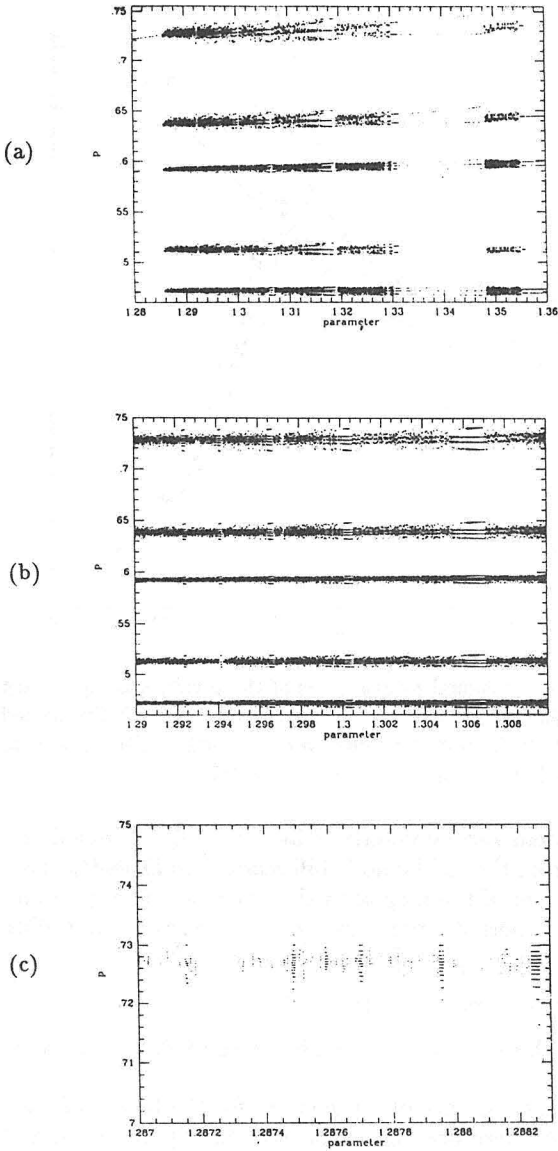


Figure 3: (a) The changes of “asymptotic” values of  $p$  at the Poincaré section for  $\epsilon_3$  belonging to  $[1.28, 1.36]$ . The 150 initial loops were omitted. Five bunches of  $p$  values corresponding to the five sets  $I_i$  are seen. (b), (c) The enlargements of two fragments of (a).

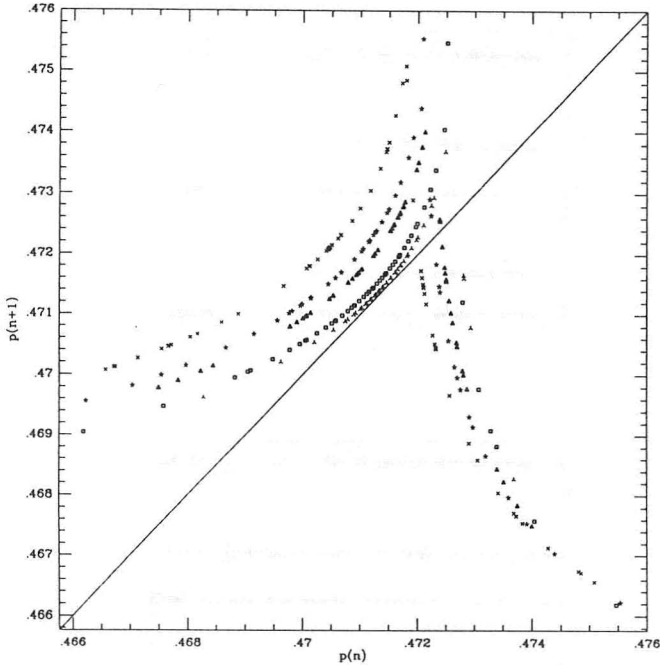


Figure 4: One-dimensional return maps of the  $p$  values along the set  $I_1$  for given values of  $\epsilon_3$ . Crosses correspond to  $\epsilon_3 = 1.32$ , five-armed stars to  $\epsilon_3 = 1.3072$ , white triangles to  $\epsilon_3 = 1.301$ , white squares to  $\epsilon_3 = 1.2904$ , and three-armed stars to  $\epsilon_3 = 1.287$ .

behavior of our system can be described by the family of one-dimensional return maps exhibiting the saddle-node bifurcation. Sufficiently close to the tangency of the branch of the map with the diagonal the appearance of an  $SSLSSL(SSLSSL)_n$ -periodic attracting orbit can be scaled according to the well-known scaling law

$$\epsilon_{3,n+1} - \epsilon_{3,n} = \text{constant}(n^{-2} - (n+1)^{-2})$$

where  $\epsilon_{3,n}$  denotes the value of  $\epsilon_3$  at which  $SSLSSL(SSLSSL)_n$ -periodic orbit appears.

The period adding sequence of bifurcations for the family of one-dimensional maps obtained here does not appear in the “pure” form as for the family of maps composed from hyperbolic curves [5,6]. The difference is that in some windows period doubling cascades are seen. This phenomenon is shown in figure 5 for the range of  $\epsilon_3$  where  $SSLSSL(SSLSSL)_3$  is attracting. The successive  $(SSLSSL(SSLSSL)_3)_{2^n}$  (for  $n = 1, 2, \dots$ ) trajectories appear.



The fifth iterate of our family of one-dimensional maps has smooth extrema around its stable fixed points and, with the change of  $\epsilon_3$ , the period doubling appears according to a well-known scenario [8].

To our best knowledge, our model is the first example of a continuous system in which the period-adding phenomenon is found. It seems, however, that the two-period-adding phenomenon has been observed in experiments. At least in two chemical systems [9,10] and in one electrochemical system [11], stable periodical oscillations of concentrations of intermediate species or electrical current with large amplitude followed by one, two, three, and so on small amplitudes appear when the appropriate bifurcation parameter is changed. These oscillations are stable in some windows of the parameter. The windows are separated by some ranges of the parameter

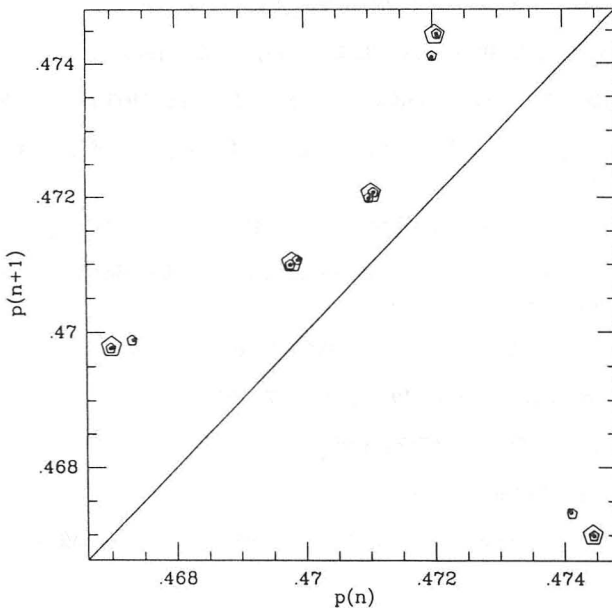


Figure 5: (a) The changes of “asymptotic” values of  $p$  at the Poincaré section for  $\epsilon_3$  belonging to  $[1.3061, 1.3068]$ . Only a subset of  $I_1$  is shown. The picture is very similar to bifurcation diagram for logistic map. The period doubling cascade is seen. (b) One-dimensional return maps for the whole set  $I_1$ .  $\epsilon_3 = 1.307$  — large pentagons correspond to the  $SSLSSL(SSLSSL)_3$  orbit,  $\epsilon_3 = 1.3064$  — medium pentagons correspond to the  $(SSLSSL(SSLSSL)_3)_2$  orbit, and  $\epsilon_3 = 1.30634$  — small pentagons correspond to the  $(SSLSSL(SSLSSL)_3)_4$  orbit.

where oscillations are chaotic. The authors do not use one-dimensional return maps to characterize these oscillations, but it seems to us that the sequence of stable periodic orbits in these systems can be described by families of one-dimensional return maps with cusp shape in the same way as in our model.

### Acknowledgments

This work was supported by the ISAS-CINECA collaborative project, under the sponsorship of the Italian Ministry for Public Education and in part by the Research Project 01.12 (Institute of Low Temperatures and Structural Researches, Polish Academy of Sciences, Wrocław). A.L.K. thanks the ISAS in Trieste for the hospitality which made this work possible.

### References

- [1] E.N. Lorenz, *J. Atmos. Sci.*, **20** (1963) 130.
- [2] F. Aicardi and A. Borsellino, *Biol. Cybernet.*, **55** (1987) 377.
- [3] J. Maselko, M. Alamgir, and J.R. Epstein, *Physica*, **19D** (1986) 153.
- [4] A.L. Kawczynski, M. Misiurewicz, and K. Leszczynski, *Pol. J. Chem.*, **63** (1989) 237.
- [5] A.L. Kawczynski and M. Misiurewicz, *Z. Phys. Chem. (Leipzig)*, in press.
- [6] M. Misiurewicz and A.L. Kawczynski, "At the other side of saddle-node," *Comm. Math. Phys.*, in press.
- [7] A.N. Tikhonov, *Mat. Sbor.*, **31** (1952) 575 (in Russian).
- [8] M.J. Feigenbaum, *J. Stat. Phys.*, **19** (1978) 25.
- [9] H.L. Swinney, *Physica*, **17D** (1986) 3.
- [10] I.R. Epstein, *Physica*, **17D** (1986) 47.
- [11] F.N. Albahadily and M. Schell, *J. Chem. Phys.*, **88** (1988) 4312.